Administration of defective virus via bang-bang optimal control inhibits dengue transmission

Tarunendu Mapder[1,2,*], John Aaskov[3], Kevin Burrage[1,2,4,*]

1 School of Mathematical Sciences, Queensland University of Technology, Brisbane, Queensland, Australia
2 Australian Research Council Centre of Excellence for Mathematical and Statistical Frontiers, Queensland University of Technology, Brisbane, Queensland, Australia
3 Institute of Health and Biomedical Innovation, Queensland University of Technology, Brisbane, Queensland, Australia
4 Department of Computer Science, University of Oxford, Oxford, UK

*** tarunendu.mapder@qut.edu.au, mtarunendu@yahoo.com, kevin.burrage@qut.edu.au**

Abstract

The host-vector shuttle and the bottleneck in dengue transmission is a significant aspect with regard to the study of dengue outbreaks. As mosquitoes require 100-1000 times more virus to become infected than human, the transmission of dengue virus from human to mosquito is a vulnerability that may be able to be targeted to improve disease control. In order to capture the heterogeneity in the infectiousness of an infected patient population towards the mosquito pool, we calibrate a population of host-to-vector virus transmission models based on an experimentally quantified infected fraction of a mosquito population. Once the population of models is well-calibrated, we deploy a population of controls that helps to inhibit the human-to-mosquito transmission of the dengue virus indirectly by reducing the viral load in the patient blood. We use an optimal bang-bang control on the administration of the defective virus (transmissible interfering particles, known as TIPs) to symptomatic patients in the course of their febrile period and observe the dynamics in successful reduction of dengue spread.

Introduction

Dengue is a major health burden in tropical regions [6, 9], which is caused by the systematic and self-limited transmission of dengue virus (DENV) between human and mosquitoes [8]. Four serotypes of the DENV arbovirus, have been identified as being transmitted by *Aedis aegypti* mosquitoes [20]. As *Aedis aegypti* is a competent vector for all serotypes of dengue virus, DENV can systematically infect and persist within the mosquito body, and eventually the vector becomes infectious [17, 21, 31, 41]. The presence of DENV in the abdomen or saliva defines a mosquito to be infected or infectious, respectively. However, the passage of DENV from the mosquito mid-gut to the salivary gland needs to cross a number of tissues barriers and innate immunity responses. To cross these hurdles, DENV needs to replicate across all the different

tissues and body fluids [15, 27]. For that reason, a bottleneck arises during the transmission flow from the human host to the mosquitoes. We suggest this phenomena as a potentially efficient dengue control.

Traditional vector controls based on reducing the mosquito population have not been successful in endemic and pandemic situations for dengue [5]. Destroying mosquito habitats using insecticides and biological controls by nematodes and fungi are primitive approaches for vector control. Due to the lack of success of these approaches [7, 42], genetic manipulation and population replacement of mosquitoes has recently been attempted [8, 18, 19]. This has not been successful due to the inability of these populations to invade the wild mosquito population. In consequence, the global spread of dengue is pandemic, accentuated, for example, through increased travel between countries and urban growth [44, 46].

Another popular control of infectious diseases spread is through vaccination. Intervention with an attenuated live virus has been successfully implemented in eradication of some diseases such as smallpox [14]. Although vaccines are available for infectious diseases including dengue, the approach has limited success due to limited vaccine coverage, obstruction in herd immunity and financial burden [2, 13, 45]. However, the most crucial reason of the failure of the conventional vaccination programs for RNA viral diseases is the frequent mutation and fast evolution rate. Thus an efficient vaccination strategy should be co-evolving and persist over passages and through the host-vector transmission shuttle.

Defective interfering viruses, containing neucleotide deletions, can be deployed as a potential co-evolving intervention. In the case of RNA viruses, defective viral genomes (DVG) are spontaneously generated within infected host cells [1, 30]. Upon infection, the positive-strand RNA appears as mRNA for translation of the replication and encapsidation machinery. The dynamic secondary and tertiary structures of positive-strand RNA play a crucial role in regulation of translation, transcription, replication and encapsidation [38]. Because of the RNA structure-mediated binding of the polymerase, 'snapback' and 'copyback' replication mechanisms generate defective genomes [36]. Within infected host cells, the defective particles interfere with virus replication and help attenuate the plasma viraemia level in the host body [22, 23]. The DI particles were so named because of the interference with the multiplication of standard virus particles. The DI particles and standard virus stimulate the host immune responses in the same way, as the DI particles are encapsidated by the normal coat proteins synthesised by the standard virus [4]. There is a large number of models studied on the generation and activities of defective interfering (DI) particles for many animal viruses [16, 28].

We have recently proposed a within-host model of dengue virus infection that covers the natural synthesis of dengue DI particles [33]. We have constructed a population of models (POMs), calibrated with clinical data for 208 patients [35]. The intention of the POMs study is to capture the biological heterogeneity in, for example, patient response, which is hard to investigate with experimental methods alone [34]. One cause of variability is the cellular infection responsible for the viral load in the patients' blood samples. Infection and super-infection by standard virus and DI particles introduce variability at numerous stages, including the membrane receptor dynamics of early-infected cells, and activation of the interferon pathways in the late-infected cells [3, 43]. Four clinically-calibrated serotype-specific POMs have been employed to investigate variability in dengue infection in physiological and pathological conditions. In the same framework, we have discussed the effect of adding excess DI particles through a bang-bang optimal control as an intervention strategy. Addition of excess DI particles to a host system that naturally generates DI particles, helps to reduce plasma viraemia peak and duration. Hence we have assigned a population of controls (POCs) for each set of POMs that produces controlled population of models (cPOMs) with lowered viraemia on successful implication. The POCs have also been characterised on the basis of its efficiency in reduction of the within-host viral burdens.

As discussed before, the transmission of dengue virus in mosquitoes is highly sensitive to the viral load of the infected patients. In this paper, we elucidate the dynamics of dengue virus transmission from infected patients into a mosquito population. Hence, we demonstrate the fraction of viral infected mosquito population, shaped by the host viraemia

profile. The time-frame of successful transmission is described at a demographic scale. We hypothesize that controlling the plasma viraemia within the infected host may efficiently restrict the host-to-vector transmission and hence the outbreak of dengue.

1 Material and Methods

The key aim of this paper is to study the transmission dynamics of DENV from human host to vector (mosquito) and the effect of adding excess DI particles on the virus transmission. To validate and calibrate the models, we utilize a set of clinical data for 208 adult dengue patients, collected by Nguyen *et. al.* in Vietnam [35]. They recorded the plasma serology profiles and quantified viraemia levels on a daily basis. In a previous study, we have deployed the patients' blood sample data to calibrate a population of within-host models (POMs) and predicted a population of personalised controls (POCs) that is able to reduce blood viraemia levels [33]. Nguyen *et. al.* also performed a mosquito exposure experiments on the same group of patients. With informed consent, each patient has been assigned for multiple exposures to mature and competent mosquitoes. About 408 exposures were scheduled purely randomly during high fever days. In each exposure, approximately 25-40 female 3-7 days old *Aedis aegypti* mosquitoes were allowed to bite on the patients' forearm. We use this dataset of mosquito exposures to help us explore the host-to-vector transmission dynamics. In this paper, we model the mosquito exposure experiment to occur in an open environment within the territory of a mosquito pool. Hence, an experimentally-calibrated population of transmission models is proposed for each DENV serotype (see 2.3 for POMs method).

1.1 Within-host Dengue Viraemia

The virus and defective particles in the patients' blood samples are used as input for the present model. The kinetics of plasma viraemia and their defective counterpart are estimated from a within-host dengue virus infection model. The within-host model describes the dynamics of cell-virus interaction and the triggered immune response inside the human host body. As the DI particles can replicate only in the dually infected cells, these cells are the only source in which to accumulate DI particles in the host blood. Hence, every time an infected host with high plasma viraemia is exposed to mosquitoes, there is a possibility that the mosquitoes when taking a blood meal are infected in three different ways: by the virus, by the DI particles or dually. As we have also predicted successful optimal bang-bang control strategy for patients' viraemia reduction, the controlled viraemia profiles are also available from the within-host model [33]. The controlled profiles are also used in the present model to observe their efficiency in transmission reduction.

1.2 Dengue Transmission In mosquitoes

With the natural birth-death flow of mosquitoes this model examines how a population of mosquitoes take blood meal from infected patients on different days during the course of their febrile period in a continuous manner. The reported data were collected on specific days, on which the mosquitoes are harvested for quantitative assays. Hence, we found a daily distribution of infected mosquitoes in order to calibrate our population of models. In general, many mathematical models of infectious disease spread follow the very well-established SIR model [26, 39]. Variants include adding compartmental models, seasonal effects and spatio-temporal dynamics [32, 37, 39]. However, tracking the transmission of the host plasma viral load to the mosquito pool within the febrile period has not yet been explored. We follow the

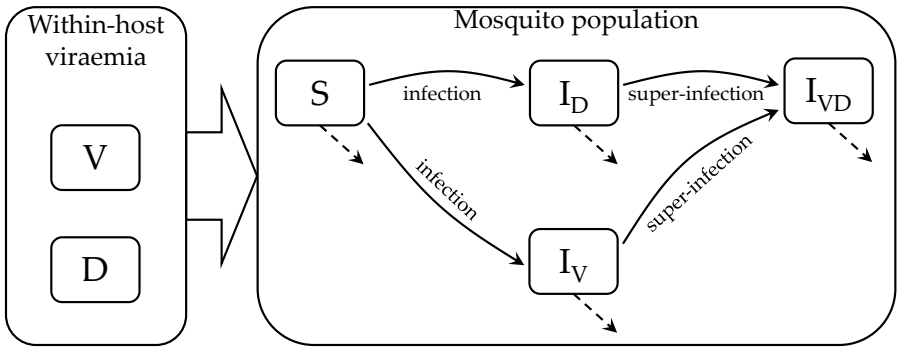

Figure 1. Schematic diagram of dengue virus transmission model: the virus (V) and the DI particles (D) are transmitted from infected hosts to mosquitoes. The susceptible mosquitoes (S) can be infected by virus or DI particles to generate the two types of infected mosquitoes, I_V and I_D. Further, a super-infected pool (I_{VD}) is generated from further infection of I_V and I_D by D and V, respectively.

traditional SIR approach but do not include the recovered (R) compartment, as mosquitoes die naturally before they can recover from dengue virus infection. We construct a population of models (see section 2.3) calibrating the range of the distribution of infectedness on each day. The transmission model utilizes the patient viremia and defective interfering (DI) particle profiles data obtained from our previous model [33]. Here, we construct the patient infectiousness model only. The model, we adopt, can explain the infected fraction of the mosquito population in terms of the transmission of viremia from the infectious patients. The model has an input of the plasma viral load from infected patient models, as shown below.

$$\begin{aligned}
\frac{dS}{dt} &= A - (\mu + \phi(V(t) + D(t)))S \\
\frac{dI_V}{dt} &= \phi S V(t) - \mu I_V \\
\frac{dI_D}{dt} &= \phi S D(t) - \mu I_D \\
\frac{dI_{VD}}{dt} &= \phi(D(t)I_V + V(t)I_D) - \mu I_{VD}.
\end{aligned} \tag{1}$$

Here, S, I_V, I_D, and I_{VD} are the susceptible and three kinds of infected pools of mature mosquitoes, respectively. The infected pools are by virus only (I_V), by DIPs only (I_D) and by both virus and DI particles (I_{VD}). A, μ and ϕ are the rate of reproduction, infection and natural death, respectively, for the mosquitoes. The plasma viral load ($V(t)$) and DI particles ($D(t)$) are obtained from our previous study [33].

1.3 Population of models

Characterising the variability between individuals from the same species is fundamental in biology. In our setting, every infected individual in a population may not produce similar infectiousness to the similar groups of susceptible, mature mosquitoes. The underlying variability may be manifested by: (1) the patients' physiology and immunological response, (2) behaviour of the uptaken virus on interaction with the host cells, (3) mosquito physiology. The first two points are covered when we use a calibrated population of patients' viral load ($V(t)$) and associated DI particles ($D(t)$). To capture the variability in patient infectiousness towards mosquitoes, a population of models approach is used for the transmission model. The main purpose of such a study is to decipher how a particular population of patients are different from the others (i.e., infectiousness to mosquitoes at different levels of viral load) and on the clinical realm, compared with the

treated (controlled) population. In a clinical and experimental framework it is difficult to track the variability, so population of mathematical models can overcome this problem even in low sample size. Two patients with similar viraemia profiles, for example, when exposed to same mosquito pools may show very different infectiousness. In such cases, the idea of a variable population of models is more realistic than a single mean-field model [10, 40].

Algorithm 1 Construction of experimentally-calibrated transmission POMs

1: *Nsample* ← number of samples
2: *Npat* ← number of within-host models in the population
3: *Nparam* ← number of model parameters
Require: *mossydata* ← **Read** human-to-mosquito transmission data files
4: *figure* ←**Draw** *mossydata* outputs
5: **for** $i \leftarrow 1, Npat$ **do**
Require: *hostmodel* ← **Read** within-host model data files
6: $t, V, D \leftarrow$ viraemia dynamics
7: *param* ← Perform LHS and build (*Nsample* × *Nparam*)-dimensional parameter hyperspace
8: **for** $j \leftarrow 1, Nsample$ **do**
9: *mossymodel*(j) ← **Solve** the model for *param*(j)
10: **if** *mossymodel*(j) ≤ range of *mossydata*(j) **then**
11: **Accept** *param*(j) into POMs
12: *figure* ← **Draw** *mossymodel*(j) outputs
13: **goto** *8*
14: **goto** *5*
15: **close**;

The population of transmission models takes the form in Eq. 1. It is calibrated by sampling the model parameters based on Latin Hypercube Sampling (LHS) [11]. Uniformly selected viremia ($V(t)$) and DI particles ($D(t)$) time profiles from the infected patients are used here as model input and the parameters (A, μ and ϕ) are sampled from Latin Hypercube Sampling. The model calibration process is based on the range of the experimental biomarker data [34]. The models, which produce the daily infected mosquito pool within the range of reported data, are included into the population from an initial population of 50,000 sampled models. We construct four separate populations of the different fractions of infected mosquitoes pool for four serotypes of DENV. Recently, we proposed an efficient calibration method by matching the distribution of the biomarker data [29]. However, here we do not calibrate the distributions due to the limited number of biomarker data variables.

2 Results

We classify the infected mosquitoes according to the nature of infecting agents as: infected by virus ($V(t)$), infected by defective particles ($D(t)$) and infected by both $V(t)$ and $D(t)$. We denote each fraction of the infected mosquitoes with respect to the entire mosquito pool as

$$\begin{aligned} \tilde{I}_V &= \frac{I_V}{(S + I_V + I_D + I_{VD})} \\ \tilde{I}_D &= \frac{I_D}{(S + I_V + I_D + I_{VD})} \\ \tilde{I}_{VD} &= \frac{I_{VD}}{(S + I_V + I_D + I_{VD})} \end{aligned} \tag{2}$$

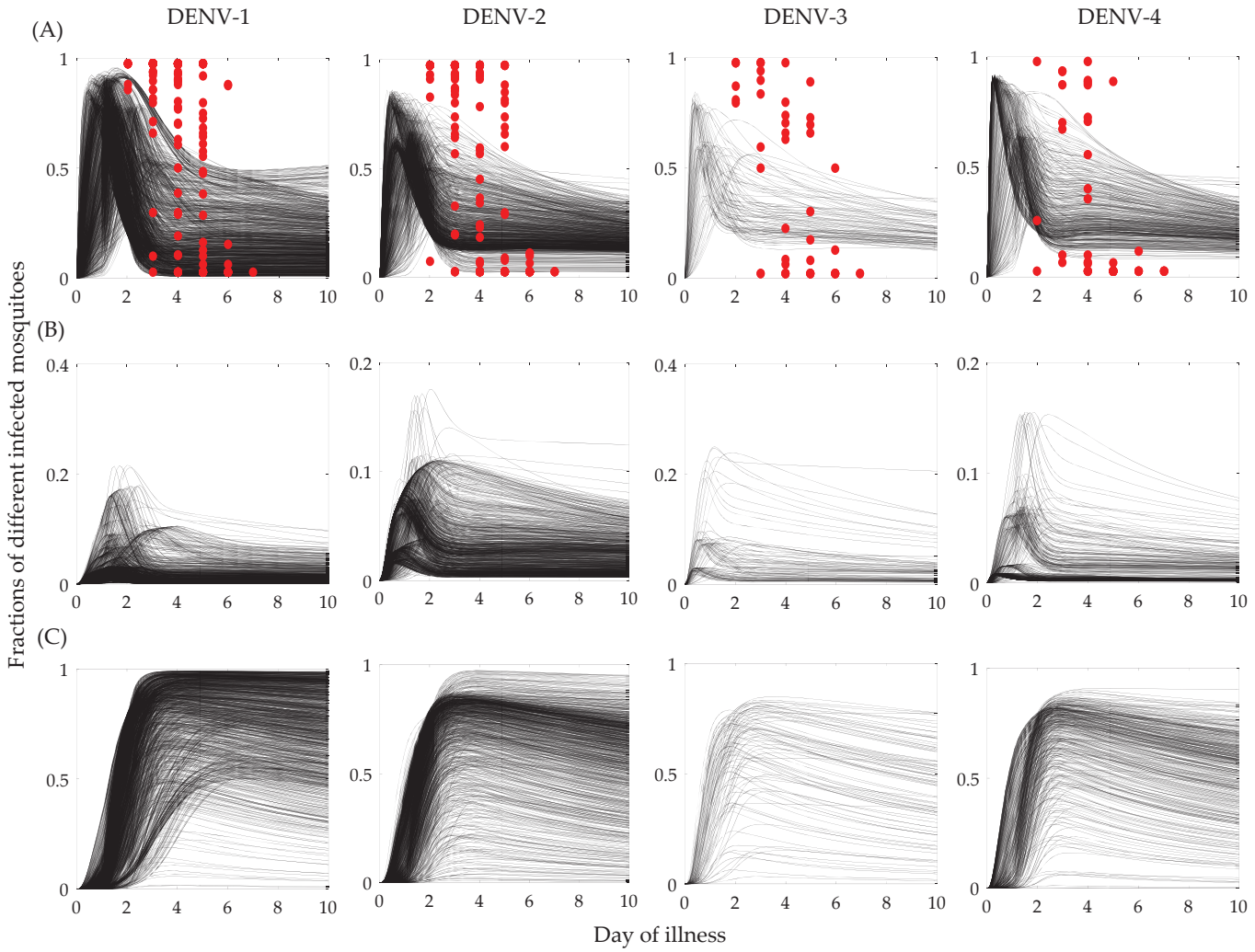

Figure 2. Population of models for infected mosquitoes: The dengue virus infected mosquito data for 408 exposure experiments with 208 hospitalised dengue patients reported in Nguyen *et al* [35] are calibrated to construct serotype-specific population of models (POMs). The biomarker data for available viral load in mosquito abdomens are shown in red dots and the calibrated models are showin in black lines. (A) infected by virus only ($\tilde{I}_V$), (B) infected by DI only ($\tilde{I}_D$), and (C) infected by both ($\tilde{I}_{VD}$) calibrated with the clinical data (red dots) and qualified models (black lines) included in the populations for four dengue serotypes: DENV-1, DENV-2, DENV-3 and DENV-4. All the data are calibrated on each day of illness.

All categories of the infected mosquitoes are shown in Fig 2. The four columns represent the infection fractions generated for four DENV serotypes. In Fig 2(A), (B), and (C), we observe $\tilde{I}_V$, $\tilde{I}_D$ and $\tilde{I}_{VD}$, respectively as described in Eq 2. The $\tilde{I}_V$ fraction is calibrated using the available clinical data, shown in red dots for 208 patients, assigned in 408 mosquito exposure experiments. On an average, every patient has been exposed twice within day 2 and day 7. The other two panels, $\tilde{I}_D$ and $\tilde{I}_{VD}$, are estimated from the simulated models. For each serotype, we simulate the same model (Eq 1) for 50,000 sampled sets of parameters from Latin Hypercube Sampling and select only those models that appear with $\tilde{I}_V$ levels within the ranges of the data. The allowed ranges of the parameters are: $A \rightarrow (5.0 \times 10^{-3} - 50.0)$, $\mu \rightarrow (2.0 \times 10^{-11} - 2.0 \times 10^{-7})$ and $\phi \rightarrow (7.5 \times 10^{-10} - 7.5 \times 10^{-6})$. The number of selected models for DENV-1, 2, 3 and 4 POMs are 1,622, 952, 89 and 387, respectively. These calibrated populations of transmission models are simulated

again with the treated viraemias. The treated viraemias are the viraemia profiles from the corresponding within-host population of models after applying the bang-bang optimal control. The controlled or treated viraemias are lower in peak height and shorter in duration than the untreated viraemias because of the addition of excess DI particles. As a result, the transmission of the viraemia into the mosquito pool are significantly low as shown in Fig 5. In Fig 3, the selected

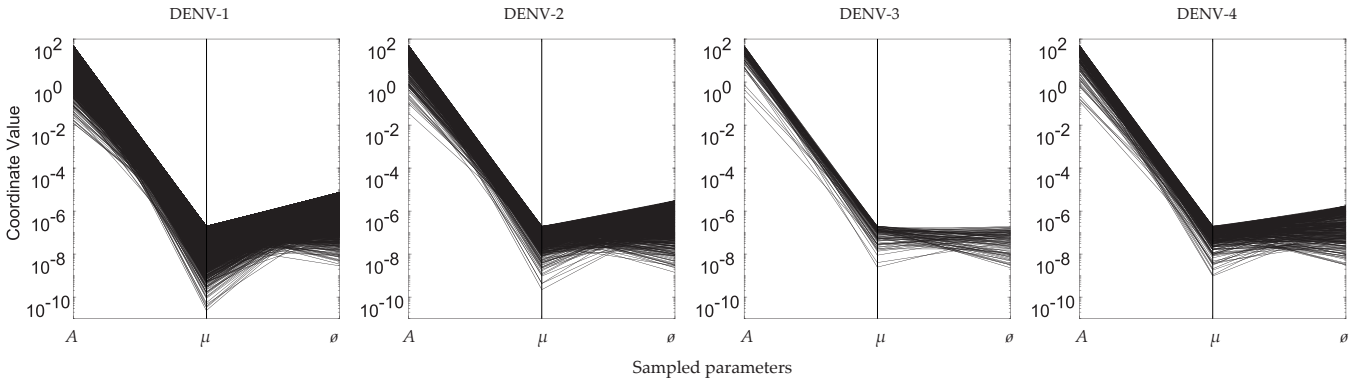

Figure 3. Variability in model parameters: The model parameters are shown in parallel co-ordinates for the four calibrated POMs of DENV-1, DENV-2, DENV-3 and DENV-4. These parameters are selected for the four serotype-specific POMs. The parameters have been sampled for 50,000 models using Latin Hypercube Sampling from a domain of 10^{-2} to 10^{2} times the initial parameter values and the qualified sets of parameters are included in the parallel co-ordinates.

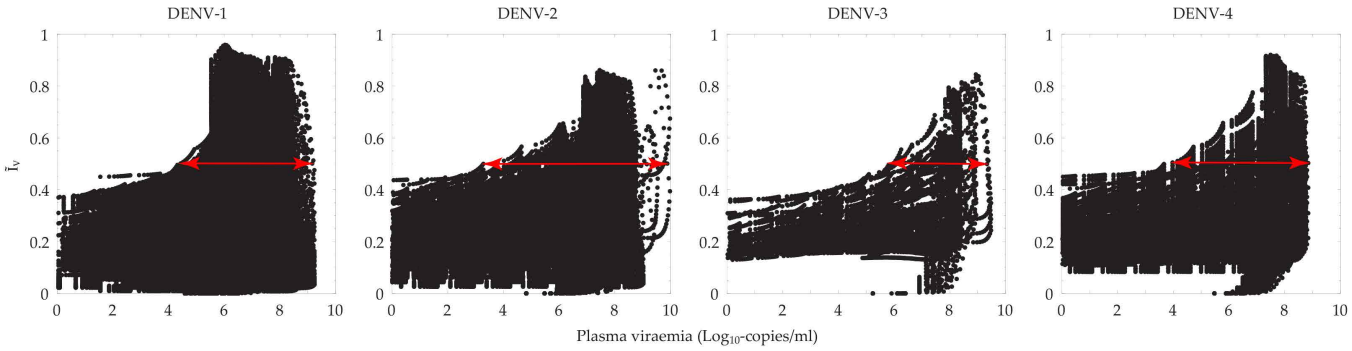

Figure 4. Mosquito infectious dose before applying control: The virus infected mosquitoes ($\tilde{I}_V$) and Log_{10} values of the corresponding patient plasma viraemia ($V(t)$) are shown in scatter plots to elucidate the ranges of the mosquito infectious dose. The viraemia responsible for 50% of mosquito infection is known as the 50% mosquito infectious dose (MID_{50}). In the figure, the whole ranges of MID_{50} (in red arrows) are plotted for the four DENV serotypes.

parameters for the calibrated models are plotted in parallel coordinates for the four dengue serotypes. A parallel coordinate graph is a geometrical model to map high-dimensional data within two-dimensions. Each data dimension appears as a vertical axis, parallel and equidistant to each other. A hyperdimensional data point is mapped as a polyline that traverses across all the axes, crossing every axis at proportional positions [24, 25]. During the calibration of POMs with the reported data, the different rate constants of mosquito reproduction (A), infection by host viraemia (ϕ) and natural mosquito death (μ) have been sampled using Latin Hypercube Sampling and selected within the POMs according to Algorithm 1.

The successful human-to-mosquito transmission of DENV has been estimated by RT-PCR (reverse transcriptase polymerase chain reaction) of the viral titre from the mosquito abdomens [35]. To correlate the patients' plasma viraemia kinetics with the mosquito infection pattern, the blood-fed mosquitoes are harvested 12 days after the day of exposure.

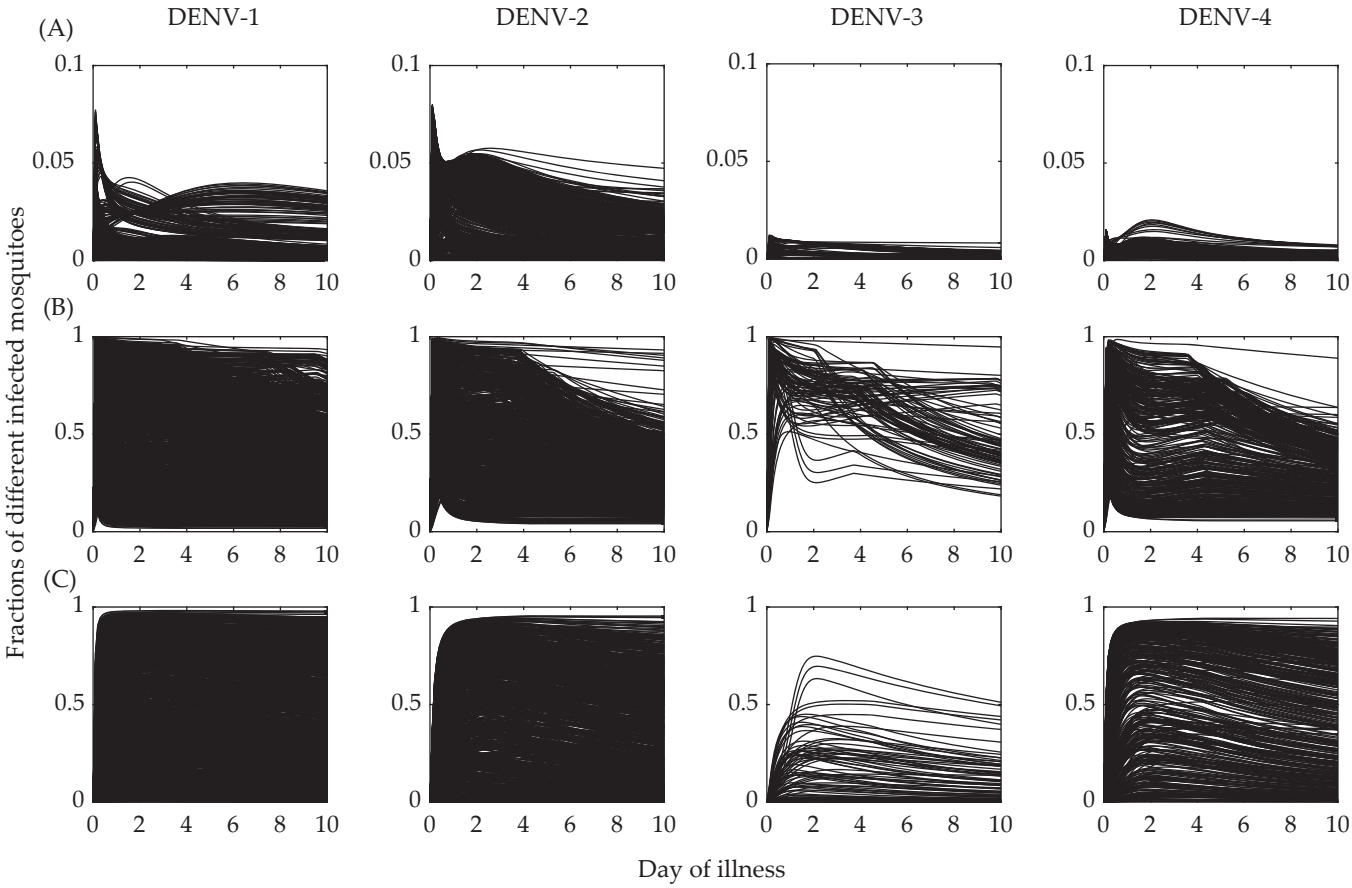

Figure 5. Controlled population of models for infected mosquitoes: Each serotype-specific POMs are considered with controlled viraemia by bang-bang control treatment with addition of excess DI particles as therapeutics. The controlled POMs (cPOMs) are presented as: (A) infected by virus only ($\tilde{I}_V$), (B) infected by DI only ($\tilde{I}_D$), and (C) infected by both ($\tilde{I}_{VD}$), simulated with the controlled within-host plasma viraemia and DI particles in the populations for four dengue serotypes: DENV-1, DENV-2, DENV-3 and DENV-4.

The efficiency of patient viraemia to infect the mosquito pool can be measured by the mosquito infectious dose (MID) in a quantitative way. The MID is a direct evaluation of the force of host-to-vector virus transmission. In the present study the plausible ranges of MIDs are estimated from the four serotype-specific calibrated POMs (Fig 4). The infected mosquito fraction ($\tilde{I}_V$) is plotted with respect to the Log10 of employed viral load ($V(t)$) from the within-host model [33]. The distribution of the 50% mosquito infectious dose (MID_{50}) is estimated for each serotypes from the fraction of $\tilde{I}_{V50}$s and the corresponding $V(t)$ levels. As a patient with high viraemia is maximally efficient for transmission, very few transmissions are observed after day 5 of illness.

In Fig 5 the POMs for the four serotypes (across the columns) simulated with the controlled viraemia from the within-host model as the input are presented. If we observe the infection in mosquitoes by the virus (Fig 5(A)), the $\tilde{I}_V$ levels for all DENV serotypes are reduced more than 10 fold. For DENV-1 and DENV-2, the overall peaks of $\tilde{I}_V$ is close to 0.05, whereas the same peaks for the uncontrolled case (Fig 2(A)) are near 0.9 and 0.85. We observe a more efficient reduction in $\tilde{I}_V$ for DENV-3 and DENV-4. The controlled $\tilde{I}_V$ for DENV-3 is below 0.01. This means the reduction in $\tilde{I}_V$ peaks are twice as effective as in DENV-1 and DENV-2. The transmission of DI infection ($\tilde{I}_D$) is increased significantly for all the serotypes, but it cannot dominate over the transmission of $\tilde{I}_{VD}$ (Fig 5(B)). The most interesting result is from

Fig 5(C) showing that the utilization of the controlled viraemia does not greatly affect co-infection ($\tilde{I}_{VD}$) profiles during the virus infection reduction. Although the co-infection population dynamics shows changes with respect to the population before intervention, the individual profiles in the whole population do not get affected. Notable reduction is observed in case of DENV-1 and DENV-3 while DENV-2 and DENV-4 are still in a good state.

Fig 6 shows the controlled ranges of mosquito infectious dose (MID) for the four DENV serotypes. In most of the cases of DENV-1 and DENV-2, the $\tilde{I}_V$ reduces with the reduction in viraemia. However, some controlled MID points are observed as outliers in the population of DENV-1 and DENV-2. If we observe these outlying points carefully, we can make a note that these points appear at the controlled peak values of the viraemias along the x-axis. The corresponding controlled $\tilde{I}_V$ fractions (see Fig 5(A)) have similar short-lived sharp peaks between day 0 and day 1 of illness. On this point we want to comment on the dengue transmission by the asymptomatic patients. For a particular value of viraemia, symptom-free dengue patients are significantly more infectious than clinically symptomatic patients [12]. Although, the outlying points in our controlled $\tilde{I}_V$ fractions are not in the region of significant transmission. On the other hand, with the same reduction in viraemia for DENV-3 and DENV-4, $\tilde{I}_V$ is reduced much more efficiently and they do not posses any such outlying points for $\tilde{I}_V$ fractions (Fig 6).

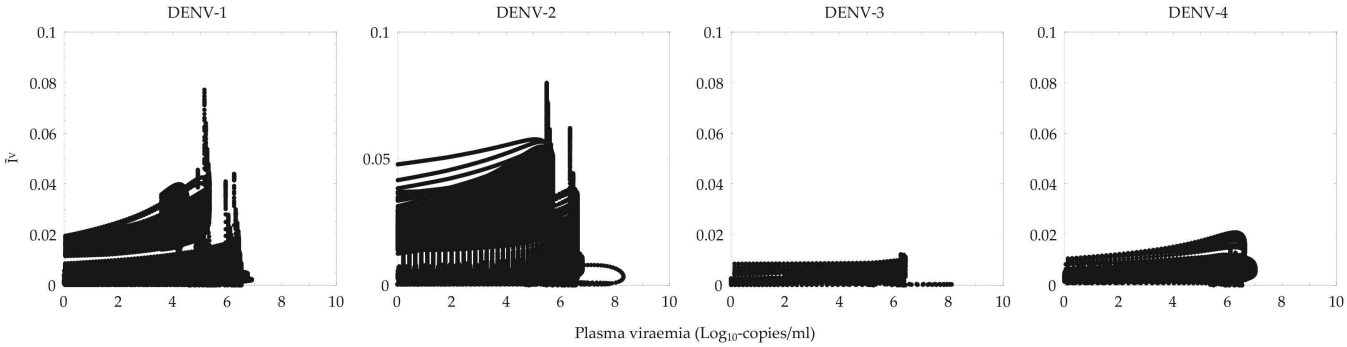

Figure 6. Controlled MIDs: The mosquito infectious doses are presented in scatter plots for the four dengue serotypes: DENV-1, DENV-2, DENV-3 and DENV-4. Scatter plots of the virus infected mosquitoes ($\tilde{I}_V$) vs Log_{10} values of the corresponding controlled patient plasma viraemia ($V(t)$) show that the probability of mosquito infection is very much low.

3 Discussion

The main goal of this paper is to calibrate a model for the infectedness of the patients to mosquito and to predict the effect of intervention with excess DI particles from the population of patients model to the mosquito transmission model. We use the method of population of models (POMs) with the viral load computed before and after applying the bang-bang control in our previous model [33]. As the reduction in virus transmission is directly related to the efficiency of the assisted transmission of DI particles, the same intervention strategy within the infected patients population may prevent the outbreak of dengue.

It is clear from Fig 2 that as long as the host viraemia level stays very high, i.e., within 2-4 days of illness, the probability of transmission into mosquitoes is high. One of the reason behind this phenomenon is the requirement of high viral load (see Fig 4) in the host blood for successful systematic replication through the tissue barriers in the mosquito body. Another reason is the shorter mosquito life cycle (approx. 15 days) that terminates mostly before the mosquito becomes infected. However, the virus assisted transmission of DI particles (I_{VD}) persists for longer, even after the virus is mostly cleared, while the only DI particles transmission is much lower than the standard virus and the assisted

transmission. We wish to explain the dynamics in terms of the replication competition in the within-host and within-vector dynamics. In the very early days of illness, the host plasma viraemia is mostly populated by the standard virus and they replicate and transmit through mosquito bites. During these days, the population of virus-infected host cells grows faster and releases virus. The DI particles and cells infected by both the standard and defective viruses appear to grow with a delay [33]. That delay is also reflected here in terms of transmission. The I_{VD} mosquito pool starts to reach high values as soon as the I_V starts to fall.

As we have discussed, the primary and secondary infections in the within-patient models can be classified with the help of their viraemia time profiles. The same situation is also reflected here in the mosquito model. As the majority of the DENV-2 and DENV-3 infected patients were diagnosed with a secondary infection, the POMs for DENV-2 and DENV-3 in the current model show sharper growth in transmission than DENV-1 and DENV-4. In contrast, the I_{VD} transmission for DENV-2 and DENV-3 are lower than that in the case of DENV-1 and DENV-4. Fig 2(C) shows the density distribution of the I_{VD} trajectories for different serotypes. These results suggests that the more secondary infections occur, the more the standard virus will be transmitted with respect to defective viruses.

The controlled profiles of the infection compartments of the mosquito pool show log scale reduction from the uncontrolled profiles. The maximum reduction is observed in the profiles of I_V after applying the control, whereas the I_{VD} profiles are not reduced completely. These results explains the underlying trade-off between the transmission of virus and DI particles. Our goal is to completely block the virus transmission with a persistent good level of DI particles transmission. However, the passage of DI particles is not possible without the assistance of the transmission of a helper virus. Hence, a high-efficiency passage of DI particles needs to allow a lower minimum level of virus to be transmitted. Nevertheless, the allowed level of viral transmission is not enough to produce dengue fever or endemic outbreak.

Although quantitative detection of the existence of viral load in different mosquito body parts is a common experiment, it is hard to detect if there exists any DI RNA. To tackle such problems, a predictive model may address a number of questions. We believe, this model is the first to explore the possible scenario of a mosquito pool, infected by blood-feeding themselves from dengue infected human host. We hope to develop another model on virus replication and the mechanism of natural occurrence of DI particles via genome deletion and mutation. This model will consider the multi-class queue of positive stranded RNA (full length and defective) and investigate the delay in terms of dengue control strategy.

Conflict of Interest Statement

The authors declare that the research was conducted in the absence of any commercial or financial relationships that could be construed as a potential conflict of interest.

Author Contributions

TM, JA and KB conceived the idea. TM and KB designed the study. TM performed the numerical experiments. TM, JA and KB analyzed the results. TM and KB wrote the manuscript. TM, JA and KB reviewed the manuscript.

Funding

This work is supported by a DARPA INTERCEPT Program (HR0011-17-2-0036).

4 Acknowledgment

We thank Nguyen et. al. for providing the data collected at the Hospital for Tropical Diseases, HCMC, Vietnam. We thank all those engaged in the DARPA INTERCEPT Dengue TIPs for suggestions and discussions. We thank the High Performance Computing (HPC) and Research Support of QUT for the computational facility.

References

1. J. Aaskov, K. Buzacott, H. M. Thu, K. Lowry, and E. C. Holmes. Long-term transmission of defective rna viruses in humans and aedes mosquitoes. *Science*, 311(5758):236–238, 2006.

2. M. Aguiar, N. Stollenwerk, and S. B. Halstead. The risks behind dengvaxia recommendation. *The Lancet infectious diseases*, 16(8):882–883, 2016.

3. M. M. Alen and D. Schols. Dengue virus entry as target for antiviral therapy. *Journal of tropical medicine*, 2012, 2012.

4. A. t. Barrett and N. Dimmock. Defective interfering viruses and infections of animals. In *Current topics in microbiology and immunology*, pages 55–84. Springer, 1986.

5. B. Beaty, S. Bernhardt, W. Black, C. Blair, L. Eisen, D. Elizondo-Quiroga, J. Farfan-Ale, S. Lozano-Fuentes, A. Franz, K. E. Olson, et al. Novel strategies to control aedes aegypti and dengue. In *Vector Biology, Ecology and Control*, pages 99–111. Springer, 2010.

6. S. Bhatt, P. W. Gething, O. J. Brady, J. P. Messina, A. W. Farlow, C. L. Moyes, J. M. Drake, J. S. Brownstein, A. G. Hoen, O. Sankoh, et al. The global distribution and burden of dengue. *Nature*, 496(7446):504, 2013.

7. J. Bisset, R. Marín, M. Rodríguez, D. Severson, Y. Ricardo, L. French, M. Díaz, and O. Pérez. Insecticide resistance in two aedes aegypti (diptera: Culicidae) strains from costa rica. *Journal of medical entomology*, 50(2):352–361, 2013.

8. C. D. Blair, Z. N. Adelman, and K. E. Olson. Molecular strategies for interrupting arthropod-borne virus transmission by mosquitoes. *Clinical microbiology reviews*, 13(4):651–661, 2000.

9. O. J. Brady, P. W. Gething, S. Bhatt, J. P. Messina, J. S. Brownstein, A. G. Hoen, C. L. Moyes, A. W. Farlow, T. W. Scott, and S. I. Hay. Refining the global spatial limits of dengue virus transmission by evidence-based consensus. *PLoS neglected tropical diseases*, 6(8):e1760, 2012.

10. O. J. Britton, A. Bueno-Orovio, K. Van Ammel, H. R. Lu, R. Towart, D. J. Gallacher, and B. Rodriguez. Experimentally calibrated population of models predicts and explains intersubject variability in cardiac cellular electrophysiology. *Proceedings of the National Academy of Sciences*, 110(23):E2098–E2105, 2013.

11. K. Burrage, P. M. Burrage, D. Donovan, T. A. McCourt, and H. B. Thompson. Estimates on the coverage of parameter space using populations of models. In *Modelling and Simulation, IASTED*. ACTA Press, 2014.

12. V. Duong, L. Lambrechts, R. E. Paul, S. Ly, R. S. Lay, K. C. Long, R. Huy, A. Tarantola, T. W. Scott, A. Sakuntabhai, et al. Asymptomatic humans transmit dengue virus to mosquitoes. *Proceedings of the National Academy of Sciences*, 112(47):14688–14693, 2015.

13. K. Fatima and N. I. Syed. Dengvaxia controversy: impact on vaccine hesitancy. *Journal of global health*, 8(2), 2018.

14. F. Fenner. Global eradication of smallpox. *Reviews of infectious diseases*, 4(5):916–930, 1982.

15. N. L. Forrester, M. Guerbois, R. L. Seymour, H. Spratt, and S. C. Weaver. Vector-borne transmission imposes a severe bottleneck on an rna virus population. *PLoS pathogens*, 8(9):e1002897, 2012.

16. S. A. Frank. Within-host spatial dynamics of viruses and defective interfering particles. *Journal of theoretical biology*, 206(2):279–290, 2000.

17. A. Franz, A. Kantor, A. Passarelli, and R. Clem. Tissue barriers to arbovirus infection in mosquitoes. *Viruses*, 7(7):3741–3767, 2015.

18. A. W. Franz, I. Sanchez-Vargas, R. R. Raban, W. C. Black IV, A. A. James, and K. E. Olson. Fitness impact and stability of a transgene conferring resistance to dengue-2 virus following introgression into a genetically diverse aedes aegypti strain. *PLoS neglected tropical diseases*, 8(5):e2833, 2014.

19. G. Fu, R. S. Lees, D. Nimmo, D. Aw, L. Jin, P. Gray, T. U. Berendonk, H. White-Cooper, S. Scaife, H. K. Phuc, et al. Female-specific flightless phenotype for mosquito control. *Proceedings of the National Academy of Sciences*, 107(10):4550–4554, 2010.

20. S. B. Halstead. Mosquito-borne haemorrhagic fevers of south and south-east asia. *Bulletin of the World Health Organization*, 35(1):3, 1966.

21. J. L. Hardy, E. J. Houk, L. D. Kramer, and W. C. Reeves. Intrinsic factors affecting vector competence of mosquitoes for arboviruses. *Annual review of entomology*, 28(1):229–262, 1983.

22. A. S. Huang and D. Baltimore. Defective viral particles and viral disease processes. *Nature*, 226(5243):325, 1970.

23. A. S. Huang and D. Baltimore. Defective interfering animal viruses. In *Comprehensive Virology 10*, pages 73–116. Springer, 1977.

24. A. Inselberg. The plane with parallel coordinates. *The visual computer*, 1:69–91, 1985.

25. A. Inselberg and B. Dimsdale. Parallel coordinates: a tool for visualizing multi-dimensional geometry. In *Proceedings of the 1st conference on Visualization'90*, pages 361–378. IEEE Computer Society Press, 1990.

26. R. Ke, J. Aaskov, E. C. Holmes, and J. O. Lloyd-Smith. Phylodynamic analysis of the emergence and epidemiological impact of transmissible defective dengue viruses. *PLoS pathogens*, 9(2):e1003193, 2013.

27. C. C. Khoo, J. Piper, I. Sanchez-Vargas, K. E. Olson, and A. W. Franz. The rna interference pathway affects midgut infection-and escape barriers for sindbis virus in aedes aegypti. *BMC microbiology*, 10(1):130, 2010.

28. T. Kirkwood and C. Bangham. Cycles, chaos, and evolution in virus cultures: a model of defective interfering particles. *Proceedings of the National Academy of Sciences*, 91(18):8685–8689, 1994.

29. B. A. Lawson, C. C. Drovandi, N. Cusimano, P. Burrage, B. Rodriguez, and K. Burrage. Unlocking data sets by calibrating populations of models to data density: A study in atrial electrophysiology. *Science advances*, 4(1):e1701676, 2018.

30. D. Li, W. B. Lott, K. Lowry, A. Jones, H. M. Thu, and J. Aaskov. Defective interfering viral particles in acute dengue infections. *PloS one*, 6(4):e19447, 2011.

31. Z. Liu, Z. Zhang, Z. Lai, T. Zhou, Z. Jia, J. Gu, K. Wu, and X.-G. Chen. Temperature increase enhances aedes albopictus competence to transmit dengue virus. *Frontiers in microbiology*, 8:2337, 2017.

32. M. Lydeamore, P. Campbell, D. Regan, S. Tong, R. Andrews, A. Steer, L. Romani, J. Kaldor, J. McVernon, and J. McCaw. A biological model of scabies infection dynamics and treatment informs mass drug administration strategies to increase the likelihood of elimination. *Mathematical biosciences*, 309:163–173, 2019.

33. T. Mapder, S. Clifford, J. Aaskov, and K. Burrage. A population of bang-bang switches of defective interfering particles makes within-host dynamics of dengue virus controllable. *PLoS computational biology*, 15(11):e1006668, 2019.

34. A. Muszkiewicz, O. J. Britton, P. Gemmell, E. Passini, C. Sánchez, X. Zhou, A. Carusi, T. A. Quinn, K. Burrage, A. Bueno-Orovio, et al. Variability in cardiac electrophysiology: using experimentally-calibrated populations of models to move beyond the single virtual physiological human paradigm. *Progress in biophysics and molecular biology*, 120(1-3):115–127, 2016.

35. N. M. Nguyen, D. T. H. Kien, T. V. Tuan, N. T. H. Quyen, C. N. Tran, L. V. Thi, D. Le Thi, H. L. Nguyen, J. J. Farrar, E. C. Holmes, et al. Host and viral features of human dengue cases shape the population of infected and infectious aedes aegypti mosquitoes. *Proceedings of the National Academy of Sciences*, 110(22):9072–9077, 2013.

36. S. Nichol, P. O'Hara, J. Holland, and J. Perrault. Structure and origin of a novel class of defective interfering particle of vesicular stomatitis virus. *Nucleic Acids Res.*, 12:2775–2790, 1984.

37. D. J. Price, N. G. Bean, J. V. Ross, and J. Tuke. Designing group dose-response studies in the presence of transmission. *Mathematical biosciences*, 304:62–78, 2018.

38. V. R. Racaniello. Picornaviridae, the virus and their replication. *Fields virology*, pages 795–838, 2007.

39. H. S. Rodrigues, M. T. T. Monteiro, and D. F. Torres. Vaccination models and optimal control strategies to dengue. *Mathematical biosciences*, 247:1–12, 2014.

40. A. X. Sarkar, D. J. Christini, and E. A. Sobie. Exploiting mathematical models to illuminate electrophysiological variability between individuals. *The Journal of physiology*, 590(11):2555–2567, 2012.

41. J. Serrato-Salas, S. Hernández-Martínez, J. Martínez-Barnetche, R. Condé, A. Alvarado-Delgado, F. Zumaya-Estrada, and H. Lanz-Mendoza. De novo dna synthesis in aedes aegypti midgut cells as a complementary strategy to limit dengue viral replication. *Frontiers in microbiology*, 9:801, 2018.

42. R. K. Singh, K. Dhama, R. Khandia, A. Munjal, K. Karthik, R. Tiwari, S. Chakraborty, Y. S. Malik, and R. Bueno-Marí. Prevention and control strategies to counter zika virus, a special focus on intervention approaches against vector mosquitoes—current updates. *Frontiers in microbiology*, 9:87, 2018.

43. J. Smit, B. Moesker, I. Rodenhuis-Zybert, and J. Wilschut. Flavivirus cell entry and membrane fusion. *Viruses*, 3(2):160–171, 2011.

44. H.-W. Tham, V. Balasubramaniam, M. K. Ooi, and M.-F. Chew. Viral determinants and vector competence of zika virus transmission. *Frontiers in microbiology*, 9, 2018.

45. L. Villar, G. H. Dayan, J. L. Arredondo-García, D. M. Rivera, R. Cunha, C. Deseda, H. Reynales, M. S. Costa, J. O. Morales-Ramírez, G. Carrasquilla, et al. Efficacy of a tetravalent dengue vaccine in children in latin america. *New England Journal of Medicine*, 372(2):113–123, 2015.

46. S. C. Weaver. Urbanization and geographic expansion of zoonotic arboviral diseases: mechanisms and potential strategies for prevention. *Trends in microbiology*, 21(8):360–363, 2013.